Spin-state crossover and low-temperature magnetic state in yttrium-doped $Pr_{0.7}Ca_{0.3}CoO_3$

K. Knížek, J. Hejtmánek, M. Maryško, P. Novák, E. Šantavá, and Z. Jirák
Institute of Physics ASCR, Cukrovarnická 10, 162 00 Prague 6, Czech Republic

T. Naito and H. Fujishiro
Faculty of Engineering, Iwate University, 4-3-5 Ueda, Morioka 020-8551, Japan

Clarina de la Cruz
Neutron Scattering Science Division, Oak Ridge National Laboratory, Oak Ridge, Tennessee 37831, USA
(Received 17 September 2013; published 11 December 2013)

The structural and magnetic properties of two mixed-valence cobaltites with a formal population of 0.30 Co^{4+} ions per f.u., $(Pr_{1-y}Y_y)_{0.7}Ca_{0.3}CoO_3$ ($y = 0$ and 0.15), have been studied down to very low temperatures by means of high-resolution neutron diffraction, SQUID magnetometry, and heat-capacity measurements. The results are interpreted within the scenario of the spin-state crossover from a room-temperature mixture of the intermediate-spin Co^{3+} and low-spin Co^{4+} (IS/LS) to the LS/LS mixture in the sample ground states. In contrast to the yttrium-free $y = 0$ that retains the metallic-like character and exhibits ferromagnetic (FM) ordering below 55 K, the doped system $y = 0.15$ undergoes a first-order metal-insulator transition at 132 K, during which not only the crossover to low-spin states but also a partial electron transfer from Pr^{3+} $4f$ to cobalt 3d states takes place simultaneously. Taking into account the nonmagnetic character of LS Co^{3+}, such a valence shift electronic transition causes a magnetic dilution, formally to 0.12 LS Co^{4+} or 0.12 t_{2g} hole spins per f.u., which is the reason for an insulating, highly nonuniform magnetic ground state without long-range order. Nevertheless, even in that case there exists a relatively strong molecular field distributed over all the crystal lattice. It is argued that the spontaneous FM order in $y = 0$ and the existence of strong FM correlations in $y = 0.15$ apparently contradict the single t_{2g} band character of LS/LS phase. The explanation we suggest relies on a model of the defect-induced, itinerant hole-mediated magnetism, where the defects are identified with the magnetic high-spin Co^{3+} species stabilized near oxygen vacancies.

DOI: 10.1103/PhysRevB.88.224412 PACS number(s): 71.30.+h, 65.40.Ba

I. INTRODUCTION

Perovskite cobaltites display a wide variety of structural and physical properties depending on the composition and temperature. Two distinct behaviors can be identified. One is characteristic for the undoped $LaCoO_3$ and its rare-earth analogs. Their insulating ground state derives from Co^{3+} ions in the diamagnetic low-spin (LS) states. With increasing temperature, two spin-state crossovers take place. First, the paramagnetic high-spin (HS) states are induced by thermal excitation and are gradually stabilized, which results in a spin-state disproportionated phase with strong HS/LS nearest-neighbor correlations or even short-range orderings,[1] which can be classified as a Mott insulator. At elevated temperature the correlations melt,[2] and a more uniform phase of quasimetallic character is established. To account for this change and to explain the paramagnetic properties actually observed, the high-temperature phase of $LaCoO_3$ was tentatively described as consisting of the intermediate spin (IS) of Co^{3+} species ($S = 1$, $m_{\text{eff}} = 2.83\mu_B$).[3–5] It should be noted, however, that dynamical mean-field theory (DMFT) calculations suggest for the high-temperature phase of $LaCoO_3$ a complex global state with the main weight of LS and HS states with only short visits to IS configurations.[6]

Another extreme case are the metallic ground states with bulk ferromagnetic (FM) ordering, known for hole-doped systems $La_{1-x}Sr_xCoO_3$ above a critical concentration $x_c = 0.22$.[7,8] Recent DMFT calculations suggest also for this case a complex distribution of local cobalt valences and spin states,[9] but with certain simplification the metallic nature of these FM phases can be related to electron transfer between neighbors of the IS Co^{3+}/LS Co^{4+} or HS Co^{3+}/HS Co^{4+} kinds, and eventually also LS Co^{3+}/LS Co^{4+}.[10] At least in the compositional region just above x_c, the $La_{1-x}Sr_xCoO_3$ systems seem to be dominated by a dynamic mixture of IS Co^{3+} and LS Co^{4+}, which is described for illustration as the IS/LS phase. This conclusion finds support among others by the observed values of ordered ferromagnetic moments, making in particular $1.70\mu_B$ per f.u. for $x = 0.30$.

When large cations in $La_{0.7}Sr_{0.3}CoO_3$ are substituted by rare-earth or calcium ions of a smaller size, the FM ordering still exists but the spontaneous moments actually observed are much suppressed. Although this effect was originally related to a phase separation into FM and non-FM, the final state at the lowest temperature is now proved, based mainly on the uniformity of a molecular field acting on Nd^{3+} moments in $Nd_{0.7}Ca_{0.3}CoO_3$,[11] to be essentially of single FM phase. The observed spontaneous moments, approaching in $Nd_{0.7}Ca_{0.3}CoO_3$ and $Pr_{0.7}Ca_{0.3}CoO_3$ a limiting low value of $0.30\mu_B$ per f.u., can thus be ascribed to a stabilization of the LS/LS phase, i.e., to the alternative ground state of the hole-doped cobaltites, which consists of a dynamic LS Co^{3+}/LS Co^{4+} mixture.

The present paper deals with $Pr_{0.7}Ca_{0.3}CoO_3$ and related compounds, $(Pr_{1-y}Y_y)_{0.7}Ca_{0.3}CoO_3$. These systems, all with 30% doping, exhibit a quasimetallic conductivity at ambient conditions, but in contrast to the formation of a FM state in pure $Pr_{0.7}Ca_{0.3}CoO_3$, the samples with partial substitution of Pr^{3+}

by isovalent Y^{3+} (for $y > 0.06$) exhibit a first-order transition to a weakly paramagnetic insulating state. Let us note that this distinct transition was observed in the 50% doped cobaltite $Pr_{0.5}Ca_{0.5}CoO_3$ upon cooling below a critical point $T_{MI} \sim 80$ K, and the change of electric properties was accompanied by important volume, magnetic, and heat-capacity anomalies.[12,13] Later on, a similar transition and anomalies were found also in other praseodymium-based systems in a larger region of doping. A question has been raised as to why a sharp transition is encountered solely in praseodymium-containing cobaltites. As suggested by generalized gradient approximation (GGA) calculations and some experimental results, including an analysis of the temperature change of interatomic lengths and x-ray-absorption near-edge structure (XANES) spectra in $Pr_{0.5}Ca_{0.5}CoO_3$, the reason for the stabilization of the insulating low-temperature phase is a shift of the mixed valence Co^{3+}/Co^{4+} toward pure Co^{3+}, enabled by a valence change of some Pr^{3+} ions to Pr^{4+} ones. The decisive factor is, therefore, the exceptional closeness in energy of the two praseodymium states. The valence shift upon phase transition has been further confirmed and determined quantitatively by observation of the Pr^{4+}-related Schottky peak in heat-capacity measurements[14] and by x-ray absorption spectroscopy at the Pr L_3 edge.[15,16] In addition to the valence shift, a crossover from the IS or mixed LS/HS Co^{3+} state to the LS states has been evidenced by a drop of the paramagnetic susceptibility and by low values of effective moments below T_{MI}, as well as by a detailed fit of the Co x-ray absorption and emission spectra.[17]

In contrast to the prototypical compound $Pr_{0.5}Ca_{0.5}CoO_3$, which is difficult to prepare because of problems with oxygen deficiency and phase separation, the less doped systems, $(Pr_{1-y}Y_y)_{0.7}Ca_{0.3}CoO_3$, appeared more suitable for experimental studies. The presence of the metal-insulator (MI) transition is demonstrated indirectly by peaks in heat capacity at $T_{MI} = 40, 64, 93$, and 132 K for $y = 0.0625, 0.075$, 0.10, and 0.15, respectively (see Fig. 1). The stabilization of tetravalent praseodymium in the low-temperature phase has been indicated by the appearance of the low-temperature Schottky peaks, arising due to Kramers degeneracy of Pr^{4+} states and Zeeman splitting of a ground doublet by the action of the molecular and external magnetic fields. The quantitative analysis determines that the Pr^{4+} population varies between

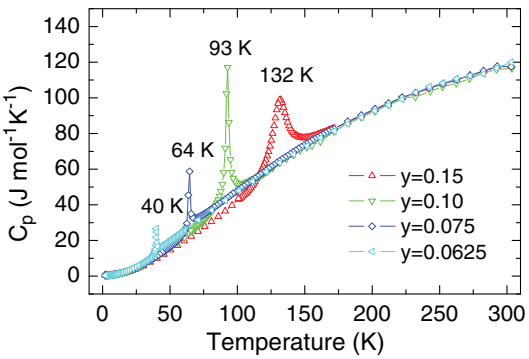

FIG. 1. (Color online) Temperature dependence of the specific heat of $(Pr_{1-y}Y_y)_{0.7}Ca_{0.3}CoO_3$ ($y = 0.0625$–0.15). The critical temperatures of the MI transitions are marked.

0.11 and 0.18 per f.u., which means that the hole concentration is decreased upon the transition from the original 30% level to 19% doping in $y = 0.0625$ and 12% doping in $y = 0.15$.[14,18] (No valence change was observed in pure $Pr_{0.7}Ca_{0.3}CoO_3$.) The motivation for the present study is to elucidate the character of the Pr^{4+} species formed below the MI transition and to investigate the microscopic origin of the unexpectedly strong molecular field of about 17 kOe, which acts on Pr^{4+} pseudospins in the low-temperature insulating phase. The study includes neutron diffraction and magnetic measurements on two selected $(Pr_{1-y}Y_y)_{0.7}Ca_{0.3}CoO_3$ samples ($y = 0$ and 0.15) down to 0.25 K.

II. EXPERIMENTS AND CALCULATIONS

$(Pr_{1-y}Y_y)_{0.7}Ca_{0.3}CoO_3$ ($y = 0$ and 0.15) samples were prepared by a solid-state reaction as described elsewhere.[18] The powder neutron diffraction was performed on the diffractometer Hb2a at Oak Ridge National Laboratory. The scans were recorded at selected temperatures between room temperature and 0.25 K. Two crystal monochromators (Ge113 and Ge115) were used, providing neutron wavelengths $\lambda = 2.408$ and 1.537 Å, respectively. Data were collected between 8° and 126° of 2θ with steps of 0.08°. Structural refinements were done by Rietveld profile analysis using the program FULLPROF (Version 5.30—Mar2012-ILL JRC).

The magnetic properties were investigated in the temperature range 2–400 K using the Quantum Design dc superconducting quantum interference device (SQUID) MPMS XL magnetometer. For the dc extraction magnetization measurements up to 140 kOe, the QD PPMS ac/dc magnetometer with the ac measurement system (ACMS) option was used. The experiments included the field-cooled (FC) and zero-field-cooled (ZFC) susceptibility scan in the range 2–300 K using a dc field of 20 Oe, together with the low-temperature measurements of virgin magnetization curves and complete hysteresis loops. In addition, the exchange bias experiments at 2 K were performed on field-cooled samples for bias fields from 500 Oe to 70 kOe. The thermoremanence was measured after cooling the sample in high field (typically 70 kOe) down to 2 K, switching off the field and scanning the magnetization at zero field on sample warming.

To determine the ground-state properties of $(Pr_{1-y}Y_y)_{0.7}Ca_{0.3}CoO_3$ cobaltites, the low-temperature magnetic contribution of the Pr^{3+} and Pr^{4+} ions was theoretically analyzed. Toward that end, the crystal-field-split $4f^n$ electronic levels were calculated using the "lanthanide" package.[19] This program takes into account the free-ion (atomic) and crystal-field terms, as well as interactions with the molecular and external magnetic fields. As far as the spherically symmetrical free-ion Hamiltonian is concerned, it depends on many parameters, the values of which are either known experimentally or may be calculated; for details, see, e.g., Ref. 20. The crystal-field Hamiltonian represents a more formidable problem. In the present case of C_s symmetry of rare-earth sites, the single-electron crystal field is described by 15 parameters. The best choice for Pr^{3+} in $(Pr_{1-y}Y_y)_{0.7}Ca_{0.3}CoO_3$ is the set of crystal-field parameters determined very recently for $PrCoO_3$ using a first-principles method.[21] The output of

the "lanthanide" calculation shows that the $^3H_4$ multiplet of Pr^{3+} ($4f^2$) splits into nine nonmagnetic singlets and the ground-state properties are manifested by anisotropic Van Vleck susceptibility with components $\chi_a = 0.0254$ emu $mol^{-1}Oe^{-1}$, $\chi_b = 0.0181$ emu $mol^{-1}Oe^{-1}$, and $\chi_c = 0.0123$ emu $mol^{-1}Oe^{-1}$ along the orthorhombic axes of the *Pbnm* structure. This yields an average value $\chi_{vV} = 0.018$ emu $mol^{-1}Oe^{-1}$ for the polycrystal, which is in excellent agreement with experimental data on a related $PrCoO_3$ system in Ref. 21, namely with its nearly temperature-independent susceptibility in the range up to $T \sim 40$ K, i.e., before the first excited level at 11 meV starts to be populated.

The calculation for Pr^{4+} (formally the $4f^1$ configuration but with a large $4f^2\underline{L}$ admixture) is subjected to more uncertainty and, moreover, there are no orthoperovskites with Pr^{4+} majority, which would allow an experimental check. As a first estimate, the values of crystal-field parameters can be taken from a very detailed optical spectroscopic study of $TbAlO_3$,[22] taking into account that this aluminate possesses the same *Pbnm* orthoperovskite structure and practically identical octahedral tilting as the present $(Pr_{1-y}Y_y)_{0.7}Ca_{0.3}CoO_3$ ($y = 0.15$) sample in the low-temperature phase. The calculation shows that the $^2F_{5/2}$ multiplet of Pr^{4+} splits into three energy distant Kramers doublets (see the Appendix of Ref. 11). The magnetic moments associated with the ground doublet ($J' = 1/2$) are given by the anisotropic g factor, with principal components $g_x = 3.757$, $g_y = 0.935$, and $g_z = 0.606$. (Here, the local axes x and y are turned with respect to the main axes of the *Pbnm* structure, making for two inequivalent rare-earth sites a rotation to $\pm 36^\circ$ around the orthorhombic axis c.)

III. RESULTS

A. Neutron diffraction study

The neutron diffraction pattern taken on $(Pr_{1-y}Y_y)_{0.7}Ca_{0.3}CoO_3$ ($y = 0$ and 0.15) is exemplified together with the FULLPROF fit in Figs. 2, 3, and 4. Although the mixed-valence cobaltites are generally subjected to an oxygen deficiency, the occupation of oxygen sites in the present two samples is surely close to the ideal stoichiometry, the refined values being 2.99 ± 0.01 and 3.01 ± 0.01 per f.u., respectively. The values of other structural parameters

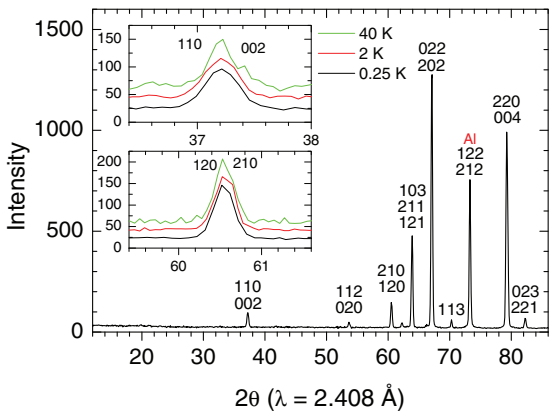

FIG. 2. (Color online) Neutron diffraction of $y = 0$ at low temperature.

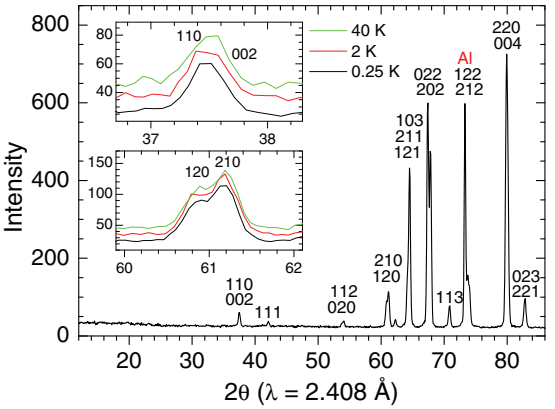

FIG. 3. (Color online) Neutron diffraction of $y = 0.15$ at low temperature.

are summarized in Tables I and II, and the unit cell volume and selected interatomic distances and angles are plotted in Figs. 5(a) and 5(b). There is little change with temperature for the $y = 0$ sample, except for common thermal expansion. In contrast, the $y = 0.15$ sample shows a marked volume compression on cooling below $T_{MI} = 132$ K, which is accompanied by an increase in the orthorhombic lattice distortion. Closer inspection reveals a larger deviation of the O-Co-O angles from the ideal 180° and some drop of the (Pr, Y, Ca)-O bonding distances, while the Co-O distances remain practically unchanged. All these signatures are manifestations of the decreased ionic size upon the $Pr^{3+} \rightarrow Pr^{4+}$ valence shift—see the similar findings for $Pr_{0.5}Ca_{0.5}CoO_3$ in Ref. 23.

As far as the magnetic state is concerned, the $y = 0$ sample shows below $T_C = 55$ K a long-range ferromagnetic (FM) order of cobalt spins that is readily seen in magnetic measurements (see below) but is barely visible in the neutron diffraction patterns as a very weak increase of some lines, mainly $110 + 002$ and $200 + 112 + 020$. The value of the spontaneous moment determined from the neutron data reaches $0.34 \pm 0.10 \mu_B$ at 0.25 K.

The detection of eventual FM ordering in $y = 0.15$ is still more difficult since the cobalt subsystem is now magnetically very dilute with only 0.12 LS Co^{4+} ions per f.u. These moments alone are below the detection limit of the neutron

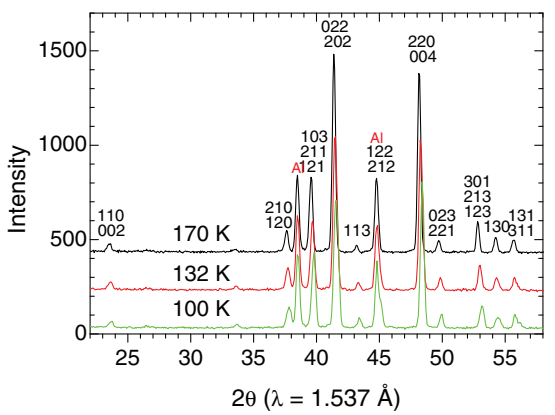

FIG. 4. (Color online) Neutron diffraction of $y = 0.15$ around the transition.

TABLE I. Structural parameters for $(Pr_{1-y}Y_y)_{0.7}Ca_{0.3}CoO_3$ with $y = 0$ within the *Pbnm* space group. Refinable atom coordinates: PrCa 4*c*(*x*,*y*,1/4), Co 4*b*(1/2,0,0), O1 4*c*(*x*,*y*,1/4), O2 8*d*(*x*,*y*,*z*).

T (K)	0.25	2	40	298
a (Å)	5.3468(2)	5.3465(2)	5.3463(4)	5.3637(2)
b (Å)	5.3359(2)	5.3353(2)	5.3352(4)	5.3516(2)
c (Å)	7.5386(3)	7.5383(2)	7.5388(5)	7.5702(4)
x,Pr	0.9952(10)	0.9949(8)	0.9953(20)	0.9934(10)
y,Pr	0.0349(7)	0.0320(5)	0.0352(16)	0.0277(4)
x,O1	0.0691(7)	0.0681(5)	0.0707(15)	0.0637(22)
y,O1	0.4920(8)	0.4910(5)	0.4924(17)	0.4901(32)
x,O2	−0.2857(8)	−0.2837(4)	−0.2879(15)	−0.2807(25)
y,O2	0.2820(9)	0.2853(3)	0.2819(18)	0.2807(25)
z,O2	0.0355(3)	0.0360(2)	0.0355(6)	0.0319(22)

diffraction, but some chance of detection is offered by very low temperatures where full alignment of Pr^{4+} moments (the $J' = 1/2$ pseudospins) due to the above-mentioned molecular field of $H_m \sim 17$ kOe could be anticipated and might add to the cobalt FM order. Nonetheless, even at 0.25 K we failed to detect any observable diffraction intensity that could prove the existence of long-range ordering in the low-temperature phase of $y = 0.15$. Let us note that for prototypical $Pr_{0.5}Ca_{0.5}CoO_3$ as well, no long-range FM order was found,[24] although the molecular field in that system is as high as $H_m \sim 75$ kOe.[14] We address this issue below and suggest an explanation.

B. Magnetic measurements

The basic magnetic characterization of the $(Pr_{1-y}Y_y)_{0.7}Ca_{0.3}CoO_3$ system was presented in our previous paper.[18] New data on ZFC/FC susceptibilities have been taken for low dc fields. The results are given in the upper panel of Fig. 6, while the lower panel illustrates the behavior in high magnetic fields. In particular, it shows the magnetization curves for the $y = 0$ and 0.15 samples, taken at 2 K in the field range 0–140 kOe and back.

The susceptibility data evidence a FM transition in the $y = 0$ sample at $T_C = 55$ K, determined by the inflection point on the fast rise of susceptibility curves, while the $y = 0.15$ sample is characterized by a drop of susceptibility that accompanies the MI transition at $T_{MI} = 132$ K. It should be noted that preformation of FM clusters at 250–270 K, reported in some recent

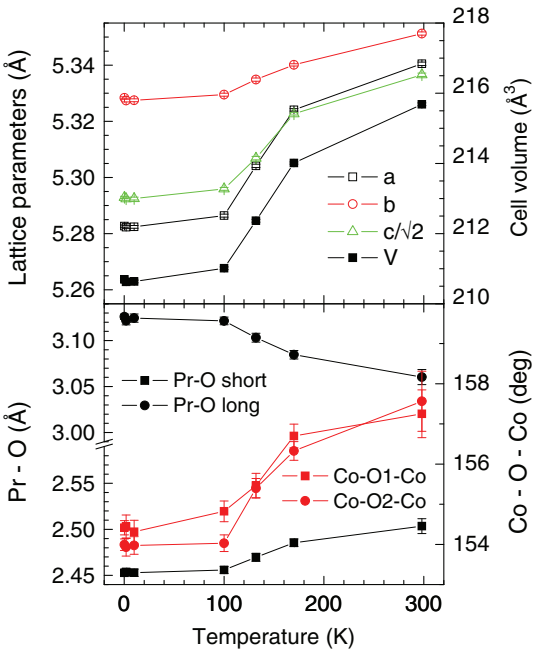

FIG. 5. (Color online) Lattice parameters and bond lengths for $y = 0.15$.

studies of similar cobaltites,[25,26] is not observed for the present samples. In particular, neither ZFC/FC bifurcation nor finite remanence extending to such high temperatures can be detected.

The magnetization data for $y = 0$ in the lower panel of Fig. 6 show a significant paraprocess that is superimposed on a hysteresis loop of relatively large coercivity (see Fig. 7) that reaches 9 kOe at 2 K. A similar paraprocess extending to very high fields has been observed also for related manganites $Pr_{0.7}Ca_{0.3}MnO_3$.[27] We thus ascribe this linear term to the Van Vleck susceptibility of Pr^{3+} and, taking experimental data on the purely LS Co^{3+} system $PrCoO_3$ in polycrystalline form as a standard, $\chi_{vv} = 0.0188$ emu mol^{-1}Oe^{-1}, or equivalently $0.0034\mu_B$/kOe,[21] we find for the valence composition $Pr^{3+}_{0.7}Ca^{2+}_{0.3}Co^{3+}_{0.7}Co^{4+}_{0.3}O^{2-}_3$ of the $y = 0$ sample a reduction of the paraprocess by a factor 0.78. This is in reasonable agreement with the actual content of 0.70 Pr^{3+}.

After subtraction of the Pr^{3+}-related paraprocess, the magnetization of the cobalt subsystem in $y = 0$, presented in Fig. 7, saturates for 140 kOe at a value of $0.58\mu_B$/Co.

TABLE II. Structural parameters for $(Pr_{1-y}Y_y)_{0.7}Ca_{0.3}CoO_3$ with $y = 0.15$ within the *Pbnm* space group. Refinable atom coordinates: PrYCa 4*c*(*x*,*y*,1/4), Co 4*b*(1/2,0,0), O1 4*c*(*x*,*y*,1/4), O2 8*d*(*x*,*y*,*z*).

T (K)	0.25	2	10	100	132	170	298
a (Å)	5.2828(4)	5.2823(5)	5.2824(5)	5.2865(5)	5.3043(6)	5.3242(4)	5.3405(6)
b (Å)	5.3285(4)	5.3273(5)	5.3275(5)	5.3296(5)	5.3349(6)	5.3401(4)	5.3513(6)
c (Å)	7.4855(6)	7.4846(7)	7.4847(7)	7.4898(8)	7.5053(9)	7.5275(6)	7.5471(8)
x,Pr	0.9924(6)	0.9902(9)	0.9898(9)	0.9933(9)	0.9937(11)	0.9949(10)	0.9966(11)
y,Pr	0.0451(3)	0.0428(6)	0.0438(6)	0.0439(5)	0.0411(6)	0.0377(5)	0.0324(2)
x,O1	0.0793(4)	0.0742(7)	0.0746(7)	0.0778(6)	0.0755(7)	0.0724(7)	0.0707(10)
y,O1	0.4873(3)	0.4861(6)	0.4864(6)	0.4872(5)	0.4883(6)	0.4900(5)	0.4928(16)
x,O2	−0.2916(3)	−0.2932(4)	−0.2929(4)	−0.2912(4)	−0.2884(4)	−0.2868(4)	−0.2848(14)
y,O2	0.2918(2)	0.2913(4)	0.2906(4)	0.2918(3)	0.2899(4)	0.2874(4)	0.2848(14)
z,O2	0.0400(2)	0.0414(3)	0.0415(3)	0.0402(3)	0.0382(3)	0.0370(3)	0.0354(10)

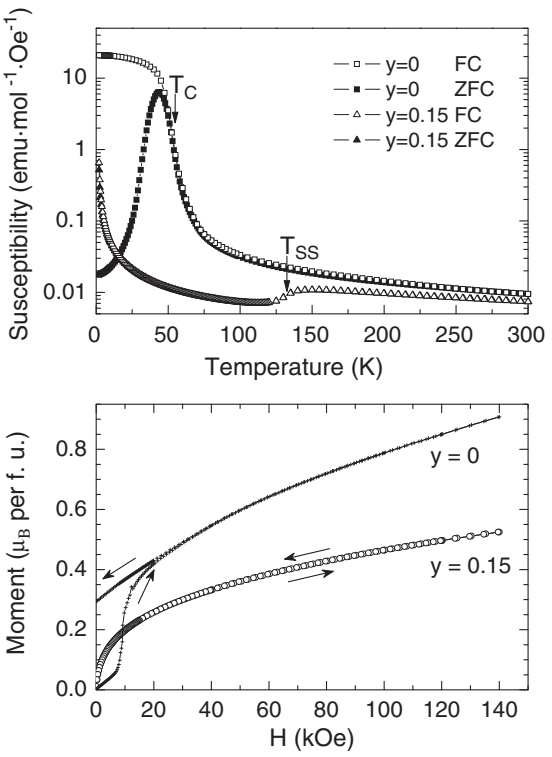

FIG. 6. Upper panel: The ZFC and FC susceptibility on $(Pr_{1-y}Y_y)_{0.7}Ca_{0.3}CoO_3$ ($y = 0$ and 0.15) measured in a dc field of 20 Oe. Note the logarithmic scale on the moment axis. Lower panel: The magnetization in fields up to 140 kOe and back, taken at 2 K.

The spontaneous moment obtained from the extrapolation to zero field is, however, lower and closely approaches the value $0.34\mu_B$, which was deduced from the neutron diffraction refinement. In our interpretation, the ground state of $Pr_{0.7}Ca_{0.3}CoO_3$ is based on the so-called LS/LS phase for Co^{3+} and Co^{4+} with a theoretical FM moment of $0.30\mu_B$/Co. With increasing external field, the IS/LS phase with a theoretical FM moment of $1.70\mu_B$/Co seems to be partially populated. For the possibility of such two-phase coexistence, see Refs. 10 and 11.

The magnetization data for the $y = 0.15$ sample reveal a highly inhomogeneous phase that can be characterized as

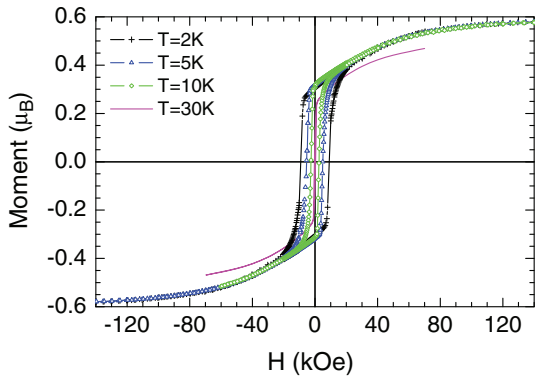

FIG. 7. (Color online) The hysteresis loops for the $Pr_{0.7}Ca_{0.3}CoO_3$ sample after subtraction of the Pr^{3+} contribution.

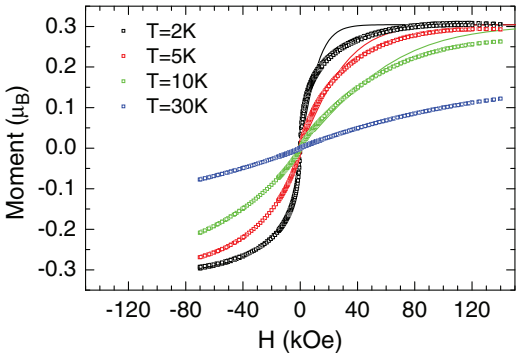

FIG. 8. (Color online) The hysteresis loops for $(Pr_{1-y}Y_y)_{0.7}Ca_{0.3}CoO_3$ ($y = 0.15$). The theoretical Brillouin curves for $S = 1/2$ and $T = 2$, 5 and 10 K are added for comparison, marked by the lines.

cluster glass with complex behaviors both in the medium and high magnetic fields. As shown in the lower panel of Fig. 6, the high-field paraprocess is reduced compared to $Pr_{0.7}Ca_{0.3}CoO_3$ and corresponds now to 0.465 of the experimental value for $PrCoO_3$. This finding is an independent confirmation of the $Pr^{3+} \rightarrow Pr^{4+}$ valence shift below T_{MI}. In fact, it is in very good quantitative agreement with the valence composition, which was deduced from Schottky peak analysis in Ref. 18—$Pr^{3+}_{0.415}Pr^{4+}_{0.18}Y^{3+}_{0.105}Ca^{2+}_{0.3}Co^{3+}_{0.88}Co^{4+}_{0.12}O^{2-}_3$.

The magnetization of $y = 0.15$ after the subtraction of the Pr^{3+} paraprocess is presented in Fig. 8. It saturates at 140 kOe on $0.30\mu_B$ per f.u., of which $0.12\mu_B$ should be attributed to the Co^{4+} contribution in the LS/LS phase and the remaining $0.18\mu_B$ is evidently the contribution of Pr^{4+} pseudospins in the $y = 0.15$ sample, supposing that the value of the $g_{J'}$ factor is close to 2. Let us note that such a value is quite reasonable in view of our theoretical estimates for Pr^{4+}, $g_x = 3.757$, $g_y = 0.935$, and $g_z = 0.606$, which yield the average value $\langle g_{J'} \rangle = 2.07$ when numerical integration over the random orientation of the crystallites is done.

The magnetization curves observed for the $y = 0.15$ sample at low temperatures deviate largely from conventional FM behavior. At first glance, the M versus H dependence is reminiscent of a paramagnet close to saturation, but compared to the standard Brillouin function the increase in low fields is steeper, suggesting the presence of large spin entities with nonuniform distribution. We estimate from the observed trend that superparamagnetic domains up to 100 cobalt ions prevail in the $y = 0.15$ sample. On the other hand, the increase in high fields is slower, suggesting strong AFM coupling between up-grown FM regions or the presence of surface states with large magnetic anisotropy as known for a so-called dead layer in nanoparticles. Upon closer inspection, one may also notice a certain opening of magnetization loops at the lowest temperatures, which is characterized by a coercive field of about 200 Oe at 2 K. A finite but very weak remanent moment of $0.014\mu_B$/Co at 2 K quickly vanishes with increasing temperature (see Fig. 9). Similar behavior has been observed also for other $(Pr_{1-y}Y_y)_{0.7}Ca_{0.3}CoO_3$ samples with a MI transition as well as for $Pr_{0.5}Ca_{0.5}CoO_3$, where the remanent moment at 2 K is, however, an order of magnitude larger.[28]

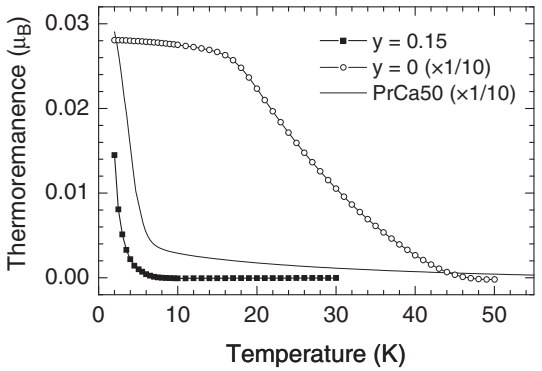

FIG. 9. The thermoremanent magnetization of $(Pr_{1-y}Y_y)_{0.7}Ca_{0.3}CoO_3$ samples. The data for $y = 0.15$ are compared with the $Pr_{0.5}Ca_{0.5}CoO_3$ sample possessing at least 20× larger thermoremanence due to excessive defects.

Another signature of the complex magnetic state of the $y = 0.15$ sample is a shift of hysteresis loops, demonstrated in Fig. 10. The effect is strongly dependent on the magnitude of the bias field.

IV. DISCUSSION

Cobaltites are highly complex systems. To understand the physical properties of mixed-valence cobaltites in the 30% doping range, at least in an illustrative way, the IS/LS scenario for Co^{3+}/Co^{4+} is generally applied. It is worth mentioning that this scenario implies carriers in two bands of very different characters and mobilities. The e_g quasiparticles are light but move in a disordered background of nearly localized t_{2g} charges and spins, and become strongly scattered, while the t_{2g} quasiparticles, although heavy and short-lived, experience a practically uniform background because of very fast fluctuations of the e_g electron subsystem. The decreased scattering in the latter case may be why the overall conductivity is likely contributed to by both the e_g and t_{2g} channels.[9] With decreasing temperature, the system $La_{0.7}Sr_{0.3}CoO_3$ of the broad e_g band maintains the IS/LS phase, whereas the narrowband

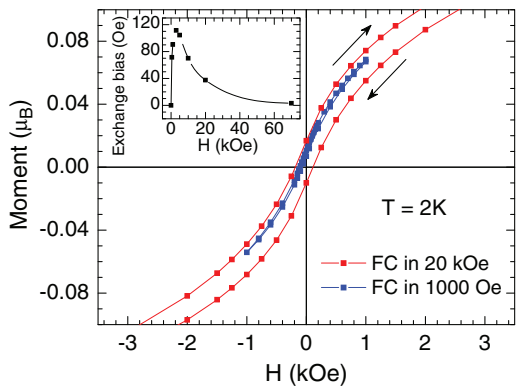

FIG. 10. (Color online) The hysteresis loops for $(Pr_{1-y}Y_y)_{0.7}Ca_{0.3}CoO_3$ ($y = 0.15$), taken at 2 K after the cooling in bias fields 1 and 20 kOe. The inset shows the bias values (the abscissa shift of the loops) in a broader range of fields.

systems such as $Pr_{0.7}Ca_{0.3}CoO_3$ or $Nd_{0.7}Ca_{0.3}CoO_3$ exhibit a gradual crossover toward lower spin states. In contrast to the true metallic conductivity of $La_{0.7}Sr_{0.3}CoO_3$, the electrical resistivity observed in $Pr_{0.7}Ca_{0.3}CoO_3$ or $Nd_{0.7}Ca_{0.3}CoO_3$ shows a steady increase with decreasing temperature but extrapolates to a finite value instead of diverging. This suggests that also in this latter case the LS/LS phase of 30% t_{2g} hole doping should be considered as intrinsically metallic.[11]

The spin-state crossover in the yttrium-containing samples $(Pr_{1-y}Y_y)_{0.7}Ca_{0.3}CoO_3$ is much more abrupt since it is accelerated by the electron transfer from Pr^{3+} to Co^{4+} at the MI transition. In the LS/LS ground state, the carrier concentration in the Co-O subsystem is thus reduced, in particular for the $y = 0.15$ sample down to 12% t_{2g} hole doping. Following the observed resistivity dependence down to 6 K, the actual regime of conduction is variable range hopping.[14,18] This means that the charge transport is realized via localized states close to the Fermi level, or, in other words, the doping level in the $y = 0.15$ sample is below the mobility edge for the t_{2g} band of the LS/LS phase.

The difference between the $y = 0$ and 0.15 samples is manifested also in their magnetic state. The $y = 0$ sample behaves at the lowest temperatures like a standard FM system with broad hysteresis loops that evidence the existence of a domain structure. The long-range magnetic order and spontaneous moments of about $0.30\mu_B$/Co are found by both neutron diffraction and magnetization measurements. We should mention, however, that the transition from the paramagnetic state is unconventional. First, no heat-capacity anomaly is observed at $T_C = 55$ K. Another feature reported in some previous studies of $Pr_{0.7}Ca_{0.3}CoO_3$ is the observation of nanosized FM objects at temperatures as high as ∼250 K. These have been detected by both small-angle neutron scattering and ZFC/FC bifurcation of the susceptibility.[25] The lack of the latter anomaly in the present study suggests that if such preformed FM objects are intrinsic to $Pr_{0.7}Ca_{0.3}CoO_3$, their size and number are likely sample-dependent.

The long-range FM order is absent in our $y = 0.15$ sample as well as in $Pr_{0.5}Ca_{0.5}CoO_3$, which is known as the prototype of the MI transition in Pr-based cobaltites. Three magnetic contributions are effective in the insulating phase of these systems: spins of LS Co^{4+}, pseudospins of the Pr^{4+} ground doublet and singlet states of Pr^{3+} with extremely large Van Vleck susceptibility $\chi_{vV} = 0.0188$ emu $mol^{-1}Oe^{-1}$, or equivalently $0.0034\mu_B$/kOe (χ_{vV} for the spin and orbital singlet LS Co^{3+} is two orders of magnitude smaller, 0.0002 emu $mol^{-1}Oe^{-1}$,[29,30] and has thus a negligible effect on the total magnetization).

It has been shown above that the paraprocess due to the Pr^{3+} contribution is simply separable, and consistent data with respect to the $Pr^{3+} \rightarrow Pr^{4+}$ valence shift are obtained. The resolution of the LS Co^{4+} and Pr^{4+} contributions appeared impossible, but their overall magnetization in Fig. 8 suggests a magnetically nonuniform phase that can be classified as the cluster glass or glassy ferromagnetism.[8] We may conclude, based on the initial slope of magnetization curves and the presence of finite thermoremanence in the $y = 0.15$ sample, that the prevailing superparamagnetic domains with easy saturation in low fields (with an average size of about 100 atoms) coexist with minor FM regions. In addition, there is

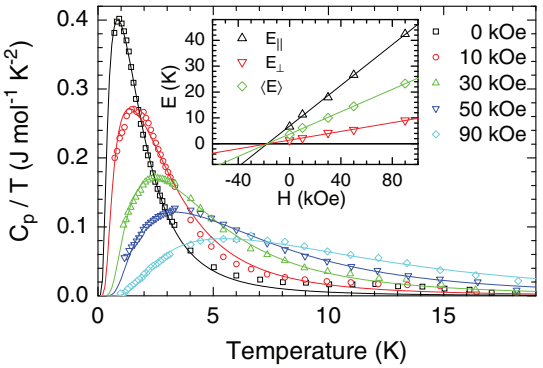

FIG. 11. (Color online) The heat capacity divided by temperature for $(Pr_{1-y}Y_y)_{0.7}Ca_{0.3}CoO_3$ ($y = 0.15$), after subtraction of lattice and nuclear terms. The full lines present the theoretical fit based on the broadening due to anisotropic Zeeman splitting, supposing the axial symmetry of the g factor. The actual values of Zeeman energy are plotted in the inset.

surely a certain population of smaller magnetic clusters or even individual spins that are manifested by the frequency-dependent ac susceptibility below 10 K (not shown here).

The pending question is the origin of the relatively strong molecular field that acts on Pr^{4+} pseudospins in the systems with the occurrence of the MI transition, in spite of the highly diluted and therefore inhomogeneously distributed Co^{4+} spins. To illustrate the problem, we revisit here the low-temperature Schottky data measured on the polycrystalline sample $y = 0.15$ in our previous paper.[18] The Schottky peaks are broadened with respect to the ideal Schottky form, but as seen in Fig. 11, an excellent fit can be obtained for the g factor of axial anisotropy, $g_\parallel = 5.86$, $g_\perp = 1.25$, irrespective of the strength of the applied field. Similar quasiaxial anisotropy of the g factor has been found in recent analysis of the Pr^{4+}-related Schottky peaks in $Pr_{0.5}Ca_{0.5}CoO_3$.[14] Important implications can be drawn from the analysis. First, the ratio $g_\parallel/g_\perp \sim= 4.7$ agrees very well with the pseudoaxial theoretical ratio for Pr^{4+}, $2g_x/(g_y + g_z) = 4.9$, suggesting that there is little or no additional inhomogeneous broadening. Hence, the Pr^{4+} pseudospins experience a molecular field of uniform strength, $H_m = 17$ kOe, although they are distributed randomly in the magnetically nonuniform phase. The origin of the molecular field should be, therefore, more complicated than in the case of Nd^{3+}-containing perovskites with a FM ground state. Second, the Schottky peak profile retains the same g-anisotropy-related broadening even at zero field, which means that the molecular field present spontaneously in the single crystal grains is not oriented along a particular crystallographic axis but behaves as in a random anisotropy system. Third, the shift of Schottky peaks with increasing external field is strictly linear, suggesting an extreme softness, which is again in variance with the behavior in FM systems with a domain structure. It is also of interest that the absolute g values deduced from the shift in applied field, in particular the average value $\langle g_{J'} \rangle = 3.22$, are much larger than the theory, and also the saturated magnetization gives ($\langle g_{J'} \rangle \sim 2$). This discrepancy suggests that there is a spin-polarizable medium in the Pr^{4+} surroundings that acts as an enhancement of the external field. This issue has been largely discussed in relation to an opposite effect in Nd-based cobaltites.[11]

V. CONCLUSIONS

Neutron diffraction and magnetic studies have been performed on two cobaltite systems $(Pr_{1-y}Y_y)_{0.7}Ca_{0.3}CoO_3$ ($y = 0$ and 0.15) with practically ideal oxygen stoichiometry. Both samples are presumably in a dynamic mixture of IS Co^{3+}/LS Co^{4+} states at room temperature and exhibit with decreasing temperature a spin-state crossover. In both cases, the ground state is identified, based on observed magnitudes of magnetic moments and robustness up to high fields, with a mixture of LS Co^{3+}/LS Co^{4+} states.

The $Pr_{0.7}Ca_{0.3}CoO_3$ sample with a formal concentration of 0.30 LS Co^{4+} in the diamagnetic background of LS Co^{3+} shows characteristics of a common FM phase ($T_C = 55$ K) with prevailing long-range order. Its electronic properties evidence the intrinsic metallicity despite the granularity of the ceramic sample.

The behavior of yttrium-substituted samples is much more complex because of a partial $Pr^{3+} \rightarrow Pr^{4+}$ and $Co^{4+} \rightarrow Co^{3+}$ valence shift, which diminishes the carrier doping in the Co-O subsystem and facilitates also the spin-state crossover to the LS/LS phase. This transition, accompanied with a drop of electrical conductivity, occurs for $y = 0.15$ at $T_{MI} = 132$ K. The transport data published earlier show that an effective conduction mechanism at the low-temperature phase is the variable range hopping, which anticipates a tunneling of t_{2g} carriers between more distant Co sites close in energy. As far as the magnetism is concerned, the present neutron diffraction, performed down to 0.25 K, does not show any long-range ordering of Co^{4+} and/or Pr^{4+} moments, and also the magnetization loops display no or a negligible opening and are characteristic rather of a glassy state. The main finding is the observation of a uniform internal field acting on Pr^{4+} pseudospins, which is surprising for the low-temperature phase of $y = 0.15$ with reduced concentration of cobalt spins (formally 0.12 LS Co^{4+} per f.u.).

The issue deserving the most attention is the origin of FM interactions that are responsible for the long-range ordering in the 30% hole-doped $Pr_{0.7}Ca_{0.3}CoO_3$ or $Nd_{0.7}Ca_{0.3}CoO_3$, as well as for the strong molecular field acting on rare-earth ions in the $(Pr_{1-y}Y_y)_{0.7}Ca_{0.3}CoO_3$ systems with severely reduced hole dopings. Regardless of the character of the LS Co^{3+}/LS Co^{4+} mixture, either localized or forming a very narrow t_{2g} band, the FM interactions in a pure phase are unlike. Namely, the superexchange interactions between LS Co^{4+} (the t_{2g}^5 configuration) should be of AFM type according to the Goodenough-Kanamori rules. In addition, when collective t_{2g} states and the single-band Hubbard model are considered, no spontaneous FM ordering can be foreseen. Neither of the double exchange interactions that are effective in the room-temperature IS/LS phase is possible. In our opinion, a possible explanation stems from magnetic defects that arise due to minor oxygen vacancies inherently present in doped cobaltites. This results in a reduced coordination of nearby cobalt ions, likely the pyramidal one, which stabilizes local HS Co^{3+} states. Their concentration is estimated based on the near oxygen stoichiometry in our samples to be $\sim 2\%$ or

less. We suggest that these very dilute defects, clearly below the percolation limit, interact ferromagnetically via itinerant t_{2g} holes. The spin polarization of the narrow t_{2g} band then mediates the nearly homogeneous molecular field over the crystal lattice.

To summarize: The sole existence of FM order in the LS/LS cobaltite phases is a general problem. Our explanation relies on a scenario of magnetic defects, which represent a nonhomogeneity but polarize t_{2g} carriers at the top of oxygen π hybridized band. Irrespective of the nature of these defects and their actual location, the spin density is thus distributed over the whole sample.

ACKNOWLEDGMENTS

We thank J. Kuneš and C. Leighton for stimulating comments. This work was supported by Project No. 204/11/0713 of the Grant Agency of the Czech Republic.

[1] J. B. Goodenough, J. Phys. Chem. Solids **6**, 287 (1958).
[2] R. A. Bari and J. Sivardiére, Phys. Rev. B **5**, 4466 (1972).
[3] T. Kyômen, Y. Asaka, and M. Itoh, Phys. Rev. B **71**, 024418 (2005).
[4] Z. Jirák, J. Hejtmánek, K. Knížek, and M. Veverka, Phys. Rev. B **78**, 014432 (2008).
[5] K. Knížek, Z. Jirák, J. Hejtmánek, P. Novák, and W. Ku, Phys. Rev. B **79**, 014430 (2009).
[6] V. Křápek, P. Novák, J. Kuneš, D. Novoselov, D. M. Korotin, and V. I. Anisimov, Phys. Rev. B **86**, 195104 (2012).
[7] R. Caciuffo, D. Rinaldi, G. Barucca, J. Mira, J. Rivas, M. A. Señarís-Rodríguez, P. G. Radaelli, D. Fiorani, and J. B. Goodenough, Phys. Rev. B **59**, 1068 (1999).
[8] J. Wu and C. Leighton, Phys. Rev. B **67**, 174408 (2003).
[9] P. Augustinský, V. Křápek, and J. Kuneš, Phys. Rev. Lett. **110**, 267204 (2013).
[10] A. O. Sboychakov, K. I. Kugel, A. L. Rakhmanov, and D. I. Khomskii, Phys. Rev. B **80**, 024423 (2009).
[11] Z. Jirák, J. Hejtmánek, K. Knížek, M. Maryško, P. Novák, E. Šantavá, T. Naito, and H. Fujishiro, J. Phys.-Condens. Matter **25**, 216006 (2013).
[12] S. Tsubouchi, T. Kyômen, M. Itoh, P. Ganguly, M. Oguni, Y. Shimojo, Y. Morii, and Y. Ishii, Phys. Rev. B **66**, 052418 (2002).
[13] S. Tsubouchi, T. Kyômen, M. Itoh, and M. Oguni, Phys. Rev. B **69**, 144406 (2004).
[14] J. Hejtmánek, Z. Jirák, O. Kaman, K. Knížek, E. Šantavá, K. Nitta, T. Naito, and H. Fujishiro, Eur. Phys. J. B **86**, 305 (2013).
[15] J. L. García-Muñoz, C. Frontera, A. J. Barón-González, S. Valencia, J. Blasco, R. Feyerherm, E. Dudzik, R. Abrudan, and F. Radu, Phys. Rev. B **84**, 045104 (2011).
[16] H. Fujishiro, T. Naito, S. Ogawa, N. Yoshida, K. Nitta, J. Hejtmánek, K. Knížek, and Z. Jirák, J. Phys. Soc. Jpn. **81**, 064709 (2012).
[17] J. Herrero-Martin, J. L. García-Muñoz, K. Kvashnina, E. Gallo, G. Subias, J. A. Alonso, and A. J. Barón-González, Phys. Rev. B **86**, 125106 (2012).
[18] J. Hejtmánek, E. Šantavá, K. Knížek, M. Maryško, Z. Jirák, T. Naito, H. Sasaki, and H. Fujishiro, Phys. Rev. B **82**, 165107 (2010).
[19] S. Edvardsson and D. Aberg, Comput. Phys. Commun. **133**, 396 (2001).
[20] S. Hufner, *Optical Spectra of Transparent Rare Earth Compounds* (Academic, New York, 1978).
[21] P. Novák, K. Knížek, M. Maryško, Z. Jirák, and J. Kuneš, J. Phys.-Condens. Matter **25**, 446001 (2013).
[22] J. B. Gruber, K. L. Nash, R. M. Yow, D. K. Sardar, U. V. Valiev, A. A. Uzokov, and G. W. Burdick, J. Lumin. **128**, 1271 (2008).
[23] A. J. Barón-González, C. Frontera, J. L. García-Muñoz, J. Blasco, and C. Ritter, Phys. Rev. B **81**, 054427 (2010).
[24] A. J. Barón-González, C. Frontera, J. L. García-Muñoz, J. Blasco, C. Ritter, S. Valencia, R. Feyerherm, and E. Dudzik, Phys. Proc. **8**, 73 (2010).
[25] S. El-Khatib, S. Bose, C. He, J. Kuplic, M. Laver, J. A. Borchers, Q. Huang, J. W. Lynn, J. F. Mitchell, and C. Leighton, Phys. Rev. B **82**, 100411 (2010).
[26] D. Phelan, Y. Suzuki, S. Wang, A. Huq, and C. Leighton, Phys. Rev. B **88**, 075119 (2013).
[27] R. M. Thomas, V. Skumryev, J. M. D. Coey, and S. Wirth, J. Appl. Phys. **85**, 5384 (1999).
[28] M. Maryško, Z. Jirák, J. Hejtmánek, and K. Knížek, J. Appl. Phys. **111**, 07E110 (2012).
[29] J. S. Griffith and L. E. Orgel, Trans. Faraday Soc. **53**, 601 (1957).
[30] H. Kamimura, J. Phys. Soc. Jpn. **21**, 484 (1966).